Accepted Manuscript

Title: Characterization of aggregates of surface modified fullerenes by asymmetrical flow field-flow fractionation with multi angle light scattering detection

Author: Alina Astefanei Wim Th. Kok Patrick Bäuerlein Oscar Núñez Maria Teresa Galceran Pim de Voogt Peter J. Schoenmakers

PII: S0021-9673(15)00955-3
DOI: http://dx.doi.org/doi:10.1016/j.chroma.2015.07.004
Reference: CHROMA 356631

To appear in: *Journal of Chromatography A*

Received date: 8-5-2015
Revised date: 30-6-2015
Accepted date: 1-7-2015

Please cite this article as: A. Astefanei, W.Th. Kok, P. Bäuerlein, O. Núñez, M.T. Galceran, P. de Voogt, P.J. Schoenmakers, Characterization of aggregates of surface modified fullerenes by asymmetrical flow field-flow fractionation with multi angle light scattering detection, *Journal of Chromatography A* (2015), http://dx.doi.org/10.1016/j.chroma.2015.07.004

This is a PDF file of an unedited manuscript that has been accepted for publication. As a service to our customers we are providing this early version of the manuscript. The manuscript will undergo copyediting, typesetting, and review of the resulting proof before it is published in its final form. Please note that during the production process errors may be discovered which could affect the content, and all legal disclaimers that apply to the journal pertain.

ACCEPTED MANUSCRIPT

- AF4-MALS for the characterization of fullerene aggregates in terms of shape and size distribution
- Study of fullerene aggregation behavior as a function of pH and ionic strength
- Carboxy-fullerenes present a stronger tendency to aggregate than polyhydroxy-fullerenes

Accepted Manuscript

*Manuscript
Click here to view linked References
ACCEPTED MANUSCRIPT

Characterization of aggregates of surface modified fullerenes by asymmetrical flow field-flow fractionation with multi angle light scattering detection

Alina Astefanei[a*], Wim Th. Kok[b], Patrick Bäuerlein[c], Oscar Núñez[a,d], Maria Teresa Galceran[a], Pim de Voogt[e], Peter J. Schoenmakers[b]

[a]Analytical Chemistry Department, University of Barcelona. Martí i Franquès 1-11, E08028 Barcelona, Spain

[b]Analytical Chemistry Department-HIMS, University of Amsterdam, PO Box 94157, 1090 GD, Amsterdam, The Netherlands

[c] KWR Watercycle Research Institute, Groningenhaven 7, P.O. Box 1072, 3430 BB, Nieuwegein, The Netherlands

[d] Serra Hunter Fellow, Generalitat de Catalunya, Spain.

[e] IBED, University of Amsterdam, PO Box 94248, 1090 GE Amsterdam, The Netherlands

* Corresponding author: Alina Astefanei

Department of Analytical Chemistry, University of Barcelona

Martí i Franquès 1-11, E-08028, Barcelona, Spain.

Phone: 34-93-402-1286

Fax: 34-93-402-1233

e-mail: astefanei.alina@gmail.com

Accepted Manuscript

ACCEPTED MANUSCRIPT

Abstract

Fullerenes are carbon nanoparticles with widespread biomedical, commercial and industrial applications. Attributes such as their tendency to aggregate and aggregate size and shape impact their ability to be transported into and through the environment and living tissues. Knowledge of these properties is therefore valuable for their human and environmental risk assessment as well as to control their synthesis and manufacture. In this work, asymmetrical flow-field flow fractionation (AF4) coupled to multi-angle light scattering (MALS) was used for the first time to study the size distribution of surface modified fullerenes with both polyhydroxyl and carboxyl functional groups in aqueous solutions having different pH (6.5-11) and ionic strength values (0-200 mM) of environmental relevance. Fractionation key parameters such as flow rates, flow programming, and membrane material were optimized for the selected fullerenes. The aggregation of the compounds studied appeared to be indifferent to changes in solution pH, but was affected by changes in the ionic strength. Polyhydroxy-fullerenes were found to be present mostly as 4 nm aggregates in water without added salt, but showed more aggregation at high ionic strength, with an up to 10-fold increase in their mean hydrodynamic radii (200 mM), due to a decrease in the electrostatic repulsion between the nanoparticles. Carboxy-fullerenes showed a much stronger aggregation degree in water (50–100 nm). Their average size and recoveries decreased with the increase in the salt concentration. This behavior can be due to enhanced adsorption of the large particles to the membrane at high ionic strength, because of their higher hydrophobicity and much larger particle sizes compared to polyhydroxy-fullerenes. The method performance was evaluated by calculating the run-to-run precision of the retention time (hydrodynamic radii), and the obtained RSD values were lower than 1 %. MALS measurements showed aggregate sizes that were in good agreement with the AF4 data. A comparison of the scattering radii from the MALS with the hydrodynamic radii obtained from the retention times in AF4 indicated that the aggregate shapes are far from spherical. TEM images of the fullerenes in the dry state also showed branched and irregular clusters.

Keywords: Asymmetrical flow field-flow fractionation; Multi angle light scattering; Fullerene aggregates

Accepted Manuscript

ACCEPTED MANUSCRIPT

1. Introduction

Fullerenes, the third carbon allotrope discovered by Kroto *et al.* in 1985 [1], are hollow-sphere nanoparticles composed entirely of carbon. Due to their unique physical and chemical properties they find widespread application in diverse fields, such as in photovoltaics [2], cosmetics [3], and biomedicine [4]. Nowadays, fullerenes functionalized with polar groups are produced in higher quantities than native fullerenes due to their increasing number of biomedical applications [5]. For instance, polyhydroxy-fullerenes have attracted attention for their good water solubility and biological compatibility [6], and have been demonstrated to be radical scavengers against superoxide anions and hydroxyl radicals [7,8]. Among these compounds, fullerol ($C_{60}(OH)_{24}$) holds a special place, being investigated for clinical application as drug carrier, tumor inhibitor [9] and mitochondrial protective antioxidant [10]. Moreover, it is being considered as starting material for synthesis of fullerene containing polymers [11] and as coating for solid-phase microextraction [12]. Carboxyl C_{60}-derivatives have potential use for photodynamic therapy [13,14] and as inhibitors of the HIV-1 protease [15].

The anticipated market growth of surface modified fullerenes, in combination with the risk of direct human exposure via several applications, has led to concerns about their potential to cause adverse effects on the environment and human health. ~~Because of their small size and large surface area to volume ratio, these compounds display a strongly elevated reactivity. It was reported that fullerol and other water soluble polyhydroxy-fullerenes are cytotoxic to human dermal fibroblast, human liver carcinoma cells and to human lens epithelial cells [16,17]. Although their acute toxicity was proved to be low, these compounds are retained in the body for long periods [18], raising concerns for chronic toxic effects.~~ However, there is a significant lack of knowledge on fullerene exposure, as well as of data on their inherent properties and toxicity. ~~The European Commission [19] and the US Environmental Protection Agency [20] have stressed the need to assess the risks posed by nanomaterials in order to produce and use these materials in a responsible way.~~

Fullerenes aggregate in aqueous media leading to the formation of ~~clusters~~ structures with various shapes and sizes. It was recently found that the size and shape of the nanoparticles formed dictate their *in vitro* toxicity [16-18] ~~[21]~~ as well as their mobility, fate, bioavailability and toxicity in the environment [19,20] ~~[22,23]~~. However, the lack of adequate methods for their

ACCEPTED MANUSCRIPT

characterization and analysis in environmental samples is currently a bottleneck in this field. Currently, the prediction of the fate and behavior of fullerenes is mostly focused on pristine compounds and is being based on laboratory experiments. A direct comparison of the data is not possible because of variations in the experimental conditions which are not consistent among studies. The data gained from the existing studies in not nearly enough to create a detailed prediction model of the behavior and fate of these nanoparticles in the environment, but represent a good starting point for their risk assessment. Therefore, it is crucial to develop reliable methods for the characterization of fullerene aggregates in terms of size distribution and shape-, at variant key environmental parameters (e.g., pH, ionic strength natural organic matter) especially for the water soluble compounds for which there is a lack of studies.

-The most commonly used techniques for particle sizing are microscopy, *e.g.*, transmission electron microscopy (TEM) or scanning electron microscopy (SEM), optical spectroscopy (UV-Vis) and light scattering techniques [21] [24]. Nonetheless, with microscopic methods the integrity of the particles and aggregates is not always guaranteed, and light-scattering methods (*e.g.*, static (MALS) and dynamic light scattering (DLS)) give average size values and are less suited to obtain information on the only instead of particle size distributions [22]. Therefore, these methods alone are often not conclusive when applied to nanoparticles and they must be combined with one or more additional methodsseparation techniques for more accurate sizing or aggregation determination [23].

FlFFF is a separation technique introduced by J. Calvin Giddings in the late seventies [24] and has become the most commonly employed mode of FFF. This is a versatile analytical tool for the separation and characterization of macromolecules and particles over a wide size range. Asymmetrical flow-field flow fractionation (AF4), including its hollow fiber format (HF5), have been the completely dominating FlFFF techniques generally used during the last decade [25]. The principles of both AF4 and FlFFF have been reviewed elsewhere [26-29]. Briefly, the fractionation principle is based on applying a perpendicular field (cross-flow) to main parabolic flow in an open flat channel. The retention of sample components of different sizes can be controlled by tuning the cross-flow rates and the separation is based on differences in the diffusion coefficients of eluting particles. The particles with larger diffusion coefficients or smaller sizes diffuse faster to upper layers inside the channel and, therefore, reach to the detector faster than the bigger ones. This is is the most widely used mechanism for analytes smaller than

Accepted Manuscript

ACCEPTED MANUSCRIPT

1 µm referred to as normal-mode separation mechanism [30]. When the particle size exceeds approximately 1 µm, the steric/hyperlayer mode prevails, and the elution order is reversed in that larger particles elute before smaller particles [31,32]. The relation between the retention time and diffusion coefficient helps in calculating hydrodynamic radii using standard AF4 theory [28,29].

Recently, AF4 was reported as a method for the size measurement of some fullerene aggregates [16,33-36] ~~[25-28]~~. Because of its versatility, this technique is used in a wide range of research and quality control applications, including nanotechnology, molecular biology and environmental analysis. Moreover, when combined with online light-scattering detection, AF4 is a powerful tool for the ~~accurate~~ determination of the size distribution of particles. For instance, Kato *et al.* [16] ~~[25]~~ studied the size distribution of aqueous C_{60} and C_{70} fullerene in a cell culture medium for *in vitro* toxicity assessment by AF4 coupled to MALS, and reported values of 256 ± 90 nm (C_{60}) and 257 ± 90 nm (C_{70}) for their diameters. Isaacson and Bouchard [33] ~~[26]~~ used AF4 coupled to dynamic light scattering (DLS) for the characterization of C_{60} fullerene aggregates in deionized water and reported hydrodynamic diameters between 80 and 260 nm. Recently, Herrero *et al.* ~~[28]~~[35] described a method for the fractionation and online identification of C_{60} and two hydrophobic C_{60}-derivatives by coupling AF4 to high resolution mass spectrometry and to MALS. The authors reported very similar size distribution for the three fullerenes, with particle radii of gyration (r_G) ranging between 20 and 80 nm. Regarding water soluble functionalized fullerenes, there are limited studies on their size distribution and aggregation behavior. AF4 with offline atomic force microscopy (AFM) was proposed for the characterization of $C_{60}(OH)_{24}$ ~~[27]~~ [34] as a function of pH and ionic strength. The authors found that fullerol ~~exists in clusters~~present aggregate sizes of only few nanometers in size (≈2 nm) at basic pH and low ionic strength. Fullerol aggregate size increased with the salt concentration from 1.8 nm at zero ionic strength up to 6.7 nm at 0.1 M NaCl, but was not affected by the pH of the solutions. These results disagree with a previous study ~~[29]~~ [37] reporting sizes on the order of 100 nm for this compound as found by dynamic light scattering and TEM. This could be due to the different methodology used for the size measurements of the particles since imaging in air induces aggregation due to partial drying of the sample before analysis.

In the present paper we describe the development and optimization of a separation method for the characterization of four surface modified fullerenes (polyhydroxy-and carboxy-derivatives) that find increasing biomedical application, in aqueous solutions by AF4 on-line

Accepted Manuscript

ACCEPTED MANUSCRIPT

coupled to UV and MALS detectors. The effect of the fractionation parameters such as carrier liquid composition, membrane material, cross flow and focus flow rate, focusing time and flow programming were evaluated. Additionally, TEM was employed to visualize the morphology and aggregate structures ion degree of the compounds studied. This research provides relevant information regarding the effect of the aqueous solution chemistry on the aggregation behavioraggregate sizes and shapes of surface modified fullerenes. in terms of shape and size distribution.

1.1 AF4 theory

Field-Flow Fractionation (FFF) is a family of separation techniques introduced by J. Calvin Giddings in 1966 the late seventies . All FFF techniques are based on the application of an external field on analyte molecules or particles that are transported by a laminar liquid flow through a thin (flat or cylindrical) channel. The field, perpendicular to the direction of the flow in the channel, forces the analyte particles into specific flow lines in the channel, with specific flow velocities. In Flow FFF the field is created by the use of a cross flow applied perpendicularly to the direction of the channel flow, through a wall that is permeable for the carrier liquid but retains the macromolecules or particles to be separated. The cross flow forces the compounds towards one of the channel walls, the accumulation wall. For each component of the sample, this accumulation is offset by a component-specific diffusive flux away from the wall. Hence, at equilibrium a size-dependent partitioning of the sample in the eluent flow profile is obtained, and sample components will be transported through the channel with a size-dependent velocity. In the first instrumental designs the channel had two porous walls passing the cross flow. In the later, asymmetrical (AF4) version, only the accumulation wall is porous, and the carrier liquid pumped into the channel is automatically split into the cross flow and the channel flow. Often, a trapezoidal shaped channel is used in AF4 to obtain a constant channel-flow along the length of the channel . AF4 has been the completely dominating Fl-FFF technique generally used during the last decade .

The retention of analyte macromolecules or particles is governed by the degree of accumulation close to the wall of the channel, which in turn is determined by the balance

Accepted Manuscript

ACCEPTED MANUSCRIPT

~~between the cross flow field and the diffusion of the analyte. For well retained analytes the retention time t_R can be predicted as:~~

$$\cancel{t_R = \frac{w^2}{6D} \ln\left(1 + \frac{F_{cr}}{F_{ch}}\right) \quad (1)}$$

~~where w is the height of the channel, F_{cr} and F_{ch} are the flow rates of the cross flow and channel flow, respectively, and D is the diffusion coefficient of the analyte particle.~~

~~The diffusion coefficient can be related to the size of the particle via the Stokes Einstein equation (for spherical particles):~~

$$\cancel{D = \frac{kT}{6\pi\eta r_H} \quad (2)}$$

~~where k is the Boltzmann constant, T the absolute temperature, η the viscosity of the solvent and r_H the hydrodynamic radius of the particle,~~

~~Thus, when the cross flow and channel flow rates are constant in the AF4 system, the particle size is a linear function of retention time and can be readily calculated from the experimental data.~~

~~For strongly polydisperse samples cross flow programming can be applied in AF4. A suitable flow program is a so-called time-delayed exponential decay (TDE) function. In TDE the cross flow is first kept constant for a certain time, and then decreased exponentially with a time constant equal to the delay time. With TDE programming, the retention time for well retained components can be approximated as:~~

$$\cancel{t_R = \tau(1 - \ln \tau + \ln t_R^*) \quad (3)}$$

~~where τ is the delay/decay time constant and t_R^* the retention time of the component with a constant flow rate. With TDE programming, the retention increases linear with the logarithm of the size of the particle.~~

Accepted Manuscript

ACCEPTED MANUSCRIPT

2. Experimental Section

2.1 Chemicals and solutions

Fullerol ($C_{60}(OH)_{24}$) was purchased from Materials & Electrochemical Research M.E.R. Corporation (Tucson, Arizona, USA). Polyhydroxy small gap fullerene, hydrated ($C_{120}(OH)_{30}$), (1,2-Methanofullerene C_{60})-61-carboxylic acid (C_{60}CHCOOH) and C_{60}-pyrrolidine tris acid (C_{60}-pyrr tris acid) were purchased from Sigma-Aldrich (Steinheim, Germany). The chemical structures and abbreviations of these compounds are given in Figure 1.

Bovine serum albumin (BSA, molecular weight ≈ 66 kDa) was purchased from Sigma-Aldrich (Steinheim, Germany). NaCl and phosphate buffered saline (PBS) were purchased from Merck (Darmstadt, Germany).

Water was purified using an Elix 3 coupled to a Milli-Q system (Millipore, Bedford, MA, USA) and filtered using a 0.22 µm nylon filter integrated into the Milli-Q system.

Stock standard solutions of polyhydroxy-fullerenes (≈1000 mg kg^{-1}) were individually prepared by weight in Milli Q water and stored at 4°C. The aqueous suspensions of both carboxy-fullerenes were obtained following the procedure proposed by Andrievsky et al., [38] with some modifications as follows: ~~by~~ first ~~dissolving~~ the solid powder was dissolved in tetrahydrofuran ~~-~~(Merck, Darmstadt, Germany), and then ~~adding~~ an exact volume of Milli Q water was added to the solution to the solution. Next, the solution was sonicated in a high power ultrasonic bath (Transonic Digital S, Elma, 40 kHz, 130 W) (Singen (Hohentwiel), Germany) until the tetrahydrofuran was completely evaporated to obtain stock solutions of approximately 500 mg kg^{-1}. Working solutions of 1 mg/mL (polyhydroxy-fullerenes) and 0.4 mg/mL (carboxy-fullerenes) were prepared weekly by appropriate dilution of the stock standard solution with Milli Q water.

2.2 Instrumentation

The optimization of the fractionation was carried out with an Eclipse Dualtec AF4 separation system (Wyatt Technology Europe GmbH, Dernbach, Germany) equipped with a programmable pump (Isocratic 1100, Agilent Technologies, Waldbronn, Germany), an Agilent 1100 series degasser and an Agilent 1200 series auto sampler/injector. A mini-channel (11cm in

Accepted Manuscript

ACCEPTED MANUSCRIPT

length, 22 mm in width at the injection point and 3 mm close to the end) was equipped with a 480 µm spacer of trapezoidal shape and Millipore regenerated cellulose (RC) membrane of 10 kDa nominal molar mass cut-~~-~~off (Superon GmbH, Dernbach, Germany). Additional experiments were conducted with Millipore 3 kDa RC and 3 and 10 kDa polyethersulfone (PES) membranes (Superon GmbH, Dernbach, Germany). Online detection was performed with a UV detector (Applied Biosystems, Foster City, California, USA). For the measurement of the r_G radii by MALS, a DAWN-DSP MALS detector (Wyatt Technology Europe GmbH, Dernbach, Germany) coupled in series to the UV detector was used. ASTRA software (Wyatt Technology) version 4.9 was used to process the data.

For TEM measurements a Jeol 1010 TEM instrument (Jeol, Japan) was used, applying an accelerating voltage of 80 kV.

2.3~~2~~ Procedures:

The calibration of FFF channel was performed by injecting 1 mg/ mL of bovine serum albumin (BSA) and using as carrier solution phosphate buffer saline (PBS) of 0.15 M at pH 7.4. From the retention data, determined from the UV signal at 280 nm, the exact channel thickness (*w*) was calculated according to the procedure described by Litzén *et al.* ~~[33]~~ [39].

The fractionations were performed in 3 steps. First, 1 µL of samples were injected in Milli Q water with an injection flow of 0.1 mL/min. Then relaxation and focusing was carried out during a specific time (3 min for the carboxy-fullerenes and 10 min for polyhydroxy-fullerenes) at a cross flow rate of 2 mL/min. Time-delayed exponential (TDE) mode was used for the elution step with a delay/decay time of 3 min (carboxy-fullerenes) and 7 min (polyhydroxy-fullerenes), an initial cross flow of 2 mL/min and a channel flow of 1 mL/min. The eluted samples were monitored by the UV detector at 254 nm and the MALS detector. The signals from the MALS ~~detec~~detector ~~tion~~ were measured simultaneously at 12 different angles (channels no. 6-17) ~~utilizes a laser source at a wavelength of 690 nm and the scattered light is measured simultaneously at 18 different angles between 17° and 155°~~ for the calculation of the radii of gyration. Angle-dependent measurements revealed a Berry model to be appropriate for evaluation of the measured values. For the normalization of the MALS channels, and to determine the inter-detector delay, a standard solution of BSA was injected. In the normalization

Accepted Manuscript

ACCEPTED MANUSCRIPT

procedure, the Stokes radius of BSA was assumed to be 3.5 nm. The experiments were conducted in a temperature controlled room (23 ± 2 °C).

.Carrier solutions with different ionic strengths (0 to 200 mM NaCl) and pH values (6.5-11) were tested to study the aggregation behavior of the fullerenes. Each carrier solutions was filtered through a 0.45 µm nylon membrane filter before use.

Diffusion coefficients and hydrodynamic radii were calculated from the observed retention times using Equations (1) and—(23).

$$t_R = \frac{w^2}{6D} \ln\left(1 + \frac{F_{cr}}{F_{ch}}\right) \qquad (1)$$

where w is the height of the channel, F_{cr} and F_{ch} are the flow rates of the cross flow and channel flow, respectively, and D is the diffusion coefficient of the analyte particle.

The (translational) diffusion coefficient can be related to the hard-sphere equivalent size of the particle via the Stokes Einstein equation for spherical particles:

$$D = \frac{kT}{6\pi\eta r_H} \qquad (2)$$

Field Cod

where k is the Boltzmann constant, T the absolute temperature, η the viscosity of the solvent and r_H the hydrodynamic radius of the particle,

Field Cod

The recovery from an AF4 run, *i*.e., the ratio between the recovered mass after analysis and injected mass, was expressed as:

$$R(\%) = \frac{A}{A_0} \times 100 \qquad (14)$$

where A and A_0 are the peak areas obtained with and without applying cross-flow, respectively. Recovery was calculated from both UV and MALS signals.

For TEM measurements, one drop of the aqueous fullerene solutions was placed on a TEM grid

Accepted Manuscript

ACCEPTED MANUSCRIPT

(carbon-coated copper grid 200 mesh (All Carbon)) and stained with a drop of uranyl formiate (1 % aqueous solution). After air drying of the grid (2 h), TEM images were taken.

3. Results and Discussion

3.1 AF4 separations ~~optimization.~~

The fractionation of fullerenes was optimized in terms of flow rates, flow programming, and focusing procedure. ~~A short (11 cm) trapezoid channel was used with a 10 kDa cutoff RC membrane in these experiments.~~ First, methods with a constant cross flow were conducted to determine flow rates that would ensure reasonable sample retention and thus the fractionation of the fullerenes studied. With a 1 mL/min channel flow, cross flow rates from 0.3 to 2.5 mL/min were tested. For the polyhydroxy-fullerenes, poor separation from the void peak at cross flow rates between 0.3 and 1.5 mL/min was observed, while with cross flows of 2 mL/min or higher, part of the fullerenes eluted only when the cross flow was stopped. Regarding the carboxy-fullerenes, their fractions could not be separated within a reasonable run time with any of the isocratic cross flow conditions tested. Therefore, flow programming was evaluated. Applying a cross flow program, with a decrease of the cross flow during the run, is a valuable tool in the AF4 separation of polydisperse samples and a simple way to expand the size window of AF4 ~~[34]~~[40]. TDE programming was used and the effect of the flow conditions (initial cross flow rate, delay/decay times) was established. Poor separation from the void peak was obtained for polyhydroxy-fullerenes in the TDE mode with initial cross flow values of 1.5 mL/min or lower, as previously observed by using the constant cross flow elution mode. Hence, a TDE program with an initial cross flow and a focus flow of 2 mL/min was used for further experiments. The best results~~-~~ (i.e., fractionation of the particles in a reasonable run time, and a good separation from the void peak) were obtained with a delay/decay time of 7 min (see Figure 2). The ~~average~~ hydrodynamic radii of the particles at the maximum of the peak height (peak-top values) were estimated from the retention time of the peaks using standard AF4 theory and the Stokes formula (Eq. ~~4~~2). For $C_{60}(OH)_{24}$ tailing peaks were observed in the fractograms obtained using UV detection, with r_H values between 3 and 30 nm and an average r_H at the maximum of the peak of approx. 4 nm (see Figure 2). The peak tailing may indicate the presence of unresolved higher

ACCEPTED MANUSCRIPT

order aggregates. The fractogram of $C_{120}(OH)_{30}$ showed a major peak corresponding to small particles with an average r_H of 4 nm and a second peak at 5 min corresponding to particles with higher degree of aggregation, with an average r_H of 12 nm. However, the retention time and the apparent size of the fullerenes in the first peak depended on the initial cross flow rate. As can be seen in Figure 3, the calculated radii of $C_{60}(OH)_{24}$ and $C_{120}(OH)_{30}$ increased from 4 nm, for cross flow values of 1.5 and 2 mL/min, to 10 nm for 2.5 mL/min. Similar behavior was observed when increasing the focus flow rate above 2 mL/min, or when increasing the focusing time. The focusing time was varied from 3 to 15 min while the other parameters (flow rates, amount of sample) were kept the same. For a good separation from the void peak for the polyhydroxy-fullerenes a minimum 10 min focusing time was required, while the r_H value found remained constant (≈ 4 nm). However, when using a 15 min focusing time, the r_H value increased to 20 nm. The observed increase in the size of the particles with the cross flow and focus flow could have its origin in particle-particle interactions, as during focusing the particles are strongly concentrated near the wall, and ~~during this step~~ particle-particle interactions may be more prominent during this step, leading to more aggregation. Although these fullerenes display elevated water solubility due to the high number of hydroxyl groups covalently bound to the C_{60} structure, they aggregate in water since the spheres tend to stick together in micelle-like aggregates [41]~~[35]~~.

For the carboxy-fullerenes the optimal fractionation conditions were a 3 min focusing time and a TDE program with an initial cross flow of 2 mL/min and a delay/decay time of 3 min. The C_{60}-pyrr tris acid fullerene eluted in at least three discernable fractions, with radii in the order of approx. 10, 30 and 95 nm, respectively (see Figure 2). For $C_{60}CHCOOH$ a small peak close to the void time was observed in the fractograms corresponding to small particles with average r_H values of 10 nm and a major peak at 7 min corresponding to larger aggregates with average r_H of 55 nm. The effect of the flow conditions (cross flow, focus flow) and focusing time on the carboxy-fullerenes was negligible, and their average radii were not affected by these experimental parameters. The effect of the cross flow on the observed r_H ~~radii~~ values of these particles is shown in Figure 3. For C_{60}-pyrr tris acid, the plotted r_H values correspond to the largest aggregates, the third peak in the fractogram (see Figure 2). Apparently, induced aggregation by the fractionation method itself does not play a major role for carboxy-fullerenes.

Membranes with different chemistries, regenerate cellulose (RC) and polyether sulphone

Accepted Manuscript

ACCEPTED MANUSCRIPT

(PES), with a molar mass cut-off of 3 and 10 kDa, were evaluated for the fractionation of the fullerenes. The relative recoveries obtained using each membrane were calculated from the total peak areas obtained with and without applying a cross flow. As can be seen in Table 1, similar relative recoveries (values between 83 and 88 %) were obtained for the polyhydroxy-fullerenes with all membranes. Slightly lower ~~recoveries~~ values were obtained for the carboxyl-fullerenes when using PES membranes compared to RC membranes. PES membranes are relatively hydrophobic (as measured by the water droplet contact angle) and they have a high negative surface charge (measured by the zeta potential), while RC membranes are more hydrophilic and have a lower negative surface charge ~~[36,37]~~[42,43]. It was previously reported that hydrophobic aromatic compounds (*e.g.*, polycyclic aromatic hydrocarbons, humic substances, aromatic pesticides) adsorb strongly on PES membranes and that the adsorption properties depend on both the hydrophobicity and molecular shape of the solutes ~~[37-41]~~[43-47]. For instance, Thang *et al.* obtained a higher recovery of isolated humic acid with a 5 kDa RC membrane than with a 2 kDa PES membrane, and found the losses to be due to adsorption of humic substances to the PES membrane ~~[40]~~[46].

The~~o~~ method reproducibility was tested by calculating the run-to-run precision. For this purpose, a total of five replicate determinations for each compound at concentration levels of 1 mg/mL were carried out on the same day (n=5). The calculated relative standard deviation (% RSD) values of the retention time at the maximum of the peak height and of the r_H were between 0.3 and 0.9 %.

3.2. AF4-MALS and TEM measurements

AF4-MALS hyphenation can offer a further insight into particle properties and can provide information on the particle size distributions as well as of the particle shape. MALS measurements can provide the radius of gyration or rms radius of particles (r_G). The r_G is defined as the mass weighted average distance from the ~~core~~ center of mass of a molecule to each mass element in the molecule and incorporates structural and shape properties of the particles. The AF4 retention time, on the other hand, provides the hydrodynamic radius r_H of a particle, which is related to its friction factor in solution. By combining the retention data from AF4 with the scattering data from the MALS detector information on the shape or architecture of particles can

Accepted Manuscript

ACCEPTED MANUSCRIPT

be obtained, by calculating a shape factor ρ, which is defined as ~~r_G/r_H~~the ratio between the scattering radii and the hydrodynamic radii. This shape factor has a value of 0.775 for spherical particles and increases as particles deviate from the spherical shape (ρ ≈ 0.8 for coils and ρ ≈ 1.7 for rods) ~~[42,43]~~[49,50].

In the present work, the AF4 instrument was coupled to MALS detection and used for the determination of the size distribution of the surface modified fullerenes and to ~~determine their shape factor~~study their shapes in aqueous solutions. Figure 4 shows the AF4-MALS fractograms obtained and the size distributions of the fullerenes studied. The 90^0 scattering signal shown in the figure was monitored for quantification. It should be noted that the scattering intensity of particles increases strongly with their size, so that the presence of larger aggregates is much emphasized in the fractograms with the light scattering signal compared to the UV signals shown in Figure 2. As can be seen in the plot, the fractionation of polyhydroxy-fullerenes revealed two resolved peaks, indicating the presence of fractions with different degree of aggregation. For $C_{60}(OH)_{24}$, the first peak close to the void time, corresponds to small aggregates with r_G of 10-40 nm and the second peak to larger aggregates with r_G of 50-60 nm. $C_{120}(OH)_{30}$ showed slightly smaller r_G with values between 10 and 30 nm (first peak) and around 40 nm (second peak). The separation of these two entities was not clear in the AF4-UV fractograms except for the peak tailing observed (Figure 2). The AF4-MALS fractograms obtained for the carboxy-fullerenes revealed in both cases a small peak corresponding to small particles with sizes lower than 20 nm and one intense and broad peak corresponding to aggregates presenting r_G ranging from 15 to 310 nm (C_{60}-pyrr tris acid) and from 20 to 310 nm (C_{60}CHCOOH), respectively.

To obtain information regarding the shapes of the aggregates, ~~The shape factor (ρ) was calculated by dividing the approximated~~ the ~~average~~ peak-top radius values obtained by MALS measurements were correlated ~~to~~ with the ~~mean~~ r_H values calculated for each peak in the fractograms at the maximum of the peak height~~for each peak in the fractograms~~. It can be noticed that the r_G values obtained for polyhydroxy-fullerenes are systematically higher than their r_H values. This could indicate that the aggregate shape of these fullerenes is far from spherical. For the carboxy-fullerenes this was not obvious, as the fractograms obtained by AF4-UV revealed several distinguishable peaks corresponding to particles of different aggregate sizes. ~~For polyhydroxy-fullerenes, values higher than 1.5 were obtained, indicating a strong deviation from the spherical particle shape. The calculated ρ values for C_{60}-pyrr tris acid were between 0.7 and~~

Accepted Manuscript

ACCEPTED MANUSCRIPT

~~1.1, for the second and third peak, respectively (Figure 2) and of approx. 1.4 for C_{60}CHCOOH pointing out the presence of both spherical particles and irregular shaped structures for these compounds.~~ Additionally, the morphology and aggregate structures of the surface modified fullerenes in water was studied by TEM and the micrographs obtained are presented in Figure 5. The images show clear differences between their aggregate structure and particle shape. In agreement with the ~~calculated ρ values~~results obtained by AF4-MALS, the images show complex branched aggregates with polycrystalline snow flake-like structures for the polyhydroxy-fullerenes which were so strongly aggregated that it was difficult to obtain an average particle size. Mostly spherical clusters and some irregular shaped structures were observed for the carboxy-fullerenes.~~, which is in agreement with the results obtained from the shape factor calculations~~. Moreover, the TEM images confirmed the polydispersity and the wide size distribution of the aggregates formed by the carboxy-fullerenes as previously observed by AF4. The micrographs revealed particles with estimated sizes between 20 and 160 nm and between 20 and 410 nm, for C_{60}-pyrr tris acid and C_{60}CHCOOH, respectively. The somewhat higher size values obtained by TEM can be due to the fact that the grids must be dried prior to imaging, and that the particles are likely to aggregate further to some degree. Nevertheless, the TEM images do provide a basis for comparison and for elucidating particle shapes and structure.

3.3. Influence of pH and ionic strength

The mobility and toxicity of fullerenes released to the environment will depend on the colloidal stability of the aggregates formed. The aggregation of these particles into larger clusters will reduce their ability to be transported or to come into contact with aquatic organisms. Knowledge of the aggregation behavior of fullerenes as a function pH and ionic strength will allow gaining an insight into their potential behavior when released in the environment. It has been reported that high ionic strength and low pH values lead to an increase in the aggregate size of C_{60} fullerene [50,51]~~[44,45]~~. Regarding surface modified fullerenes, previous studies have shown that fullerol aggregation is also promoted by an increase in the ionic strength and that it is not affected by the pH variation ~~[27,45]~~ [34,51]. In this work, the behavior of the fullerenes studied was evaluated at different ionic strength (0-200 mM) and pH values (6.5-11). These values were chosen as they include the normal range of the pH of surface and sea waters (6.5-

Accepted Manuscript

ACCEPTED MANUSCRIPT

8.5) and their usual salt concentration (1-500 mM). No significant changes in the size of the particles were observed when varying the pH between 6.5 and 11. Apparently, within this pH range fullerene clusters maintain a substantial charge, which is in agreement with previous reports [34,37]~~[27,29]~~. In Figure 6 the influence of the ionic strength on the average hydrodynamic radii of the particles is shown. The hydrodynamic radius of polyhydroxy-fullerene aggregates increases significantly with the ionic strength. The mean radius of $C_{120}(OH)_{30}$ and $C_{60}(OH)_{24}$ increased from approximately 4 nm at zero ionic strength up to 40 nm and 50 nm, respectively, in 200 mM salt concentration. At the same time, an increase in their r_G with the ionic strength was observed in AF4-MALS measurements. As an example, Figure 7 shows the fractograms and size distribution obtained by MALS for $C_{60}(OH)_{24}$ at 0 and 30 mM salt concentrations. The change in the elution profile (retention time shift) with higher salt concentration is accompanied by an increase in r_G, up to 160 nm in a solution containing 30 mM NaCl. This behavior is in agreement with the findings in previous studies ~~[27,29]~~[34,37] and with the Derjaguin–Landau–Verwey–Overbeek (DLVO) theory which is commonly used to describe interactions of charged surfaces across liquids [52]~~[46]~~. The increase in the ionic strength showed a different effect for the carboxy-fullerenes. A slight decrease in the average hydrodynamic radii of both C_{60}CHCOOH and C_{60}-pyrr tris acid with an increase in NaCl concentration was observed, from 55 and 95 nm, respectively, at zero ionic strength to 45 and 65 nm, respectively, in 200 mM NaCl (Figure 6). In agreement with these results, their r_G as obtained by MALS also slightly decreased. Moreover, the increase in the ionic strength of the solution caused a significant decrease in the peak areas of the carboxy-fullerenes. Figure 8 shows the relative recoveries of these compounds from the channel at different salt concentrations. A possible explanation for the low recovery of the carboxy-fullerenes at high salt concentration (less than 20 % for 200 mM NaCl) could be an enhanced adsorption of these particles to the membrane. Due to their higher hydrophobicity and larger size, membrane adsorption of carboxy fullerenes is more likely compared to the polydroxy-fullerenes. This assumption was further confirmed by the appearance of a brown spot in the focusing area of the AF4 membrane after repeated injections. Particle adsorption on the accumulation wall in AF4 is governed by the attractive van der Waals forces and the electrostatic repulsion between particles and the membrane surface, which will decrease with increasing salt concentration ~~[47-49]~~[53-55]. In other studies it has been reported that the increase in the salt content reduces the zeta potential of

Accepted Manuscript

ACCEPTED MANUSCRIPT

RC membrane which lowers the electrostatic forces between nanoparticles and the RC membrane, leading to increased adsorption ~~[50,51]~~[56,57].

4. Conclusions:

The chemical derivatization of fullerenes with different polar functional groups has an effect on the agglomeration state of the particles in aqueous solutions and therefore could affect their environmental behavior. In this study, ~~it was shown that~~ AF4-MALS was used ~~is a suitable technique~~ to ~~assess~~ determine the aggregate sizes~~ion~~ ~~behavior~~ of surface modified fullerenes. With a 10 kDa cut-off RC membrane in the AF4 channel good relative recovery values (79-85 %) were obtained for the fullerenes studied. The application of TDE cross flow programming enabled the separation of aggregates with sizes (hydrodynamic radii) from approximately 4 nm to well over 100 nm. It was found that polyhydroxy-fullerenes are present in pure water as small aggregates with hydrodynamic radii in the order of 4–15 nm. Only a small fraction of these fullerenes is present in larger agglomerates. Experiments with high cross flows and/or long focusing times indicated that the aggregation as found experimentally may be partly induced by the focusing process, in which the fullerenes are strongly concentrated. The pH of the solution did not affect their aggregation. On the other hand, the ionic strength of the solution was found to be an important factor. In the presence of sodium chloride (30–200 mM) a much larger fraction of the polyhydroxy-fullerenes was found in aggregates with radii in the order of 40–60 nm. The carboxy-fullerenes studied showed a much stronger tendency to aggregate than the polyhydroxy-fullerenes. Even in water without added salt, their aggregation radius was around 55 nm and 95 nm. With the addition of salt to the solution a small decrease of their average aggregate size was found. However, at higher ionic strength the recovery of the carboxy-fullerenes from the AF4 channel was strongly decreased. This can possibly be attributed to an increased adsorption of the (fairly hydrophobic) fullerenes to the membrane material. When this adsorption would be size-dependent, the observed decrease of the average aggregate size could be related to this. Data obtained from the MALS detector coupled on-line to the AF4 instrument largely confirmed the aggregate size distributions as calculated from the fractograms. The shape factors for the aggregates, obtained by comparing the scattering radii from the MALS data with the hydrodynamic radii from the elution times, indicate that the aggregates of (polyhydroxy-)

Accepted Manuscript

ACCEPTED MANUSCRIPT

fullerenes are not spherical but strongly branched. TEM measurements confirmed this observation.

The methodology developed in this study can guide future work for the characterization of fullerenes, to study their aggregation behavior in aqueous media and hence to improve the understanding of the fate of these particles in the environment.

Acknowledgments

The authors gratefully acknowledge for the financial support received from the Spanish Ministry of Economy and Competitiveness under the project CTQ2012-30836, and from the Agency for Administration of University and Research Grants (Generalitat de Catalunya, Spain) under the project 2014 SGR-539. Alina Astefanei acknowledges the Spanish Ministry of Economy and Competitiveness for a Ph.D. grant (FPI-MICINN) which enabled her to carry out this research as a visiting scientist at the University of Amsterdam. Part of this work was supported by the Joint Research Program of the Dutch Water Utilities (BTO, The Netherlands). We also thank Carmen Lopez and Nieves Hernandez (CCiTUB, University of Barcelona) for help with the TEM analysis.

Accepted Manuscript

ACCEPTED MANUSCRIPT

Figure captions:

Figure 1. Structure of the surface modified fullerenes studied.

Figure 2. AF4-UV fractograms of the surface modified fullerenes. TDE flow programming with a delay/decay time of 7 min (a and b) or 3 min (c and d). For experimental conditions see text. (a) $C_{60}(OH)_{24}$; (b) $C_{120}(OH)_{30}$; (c) C_{60}-pyrr tris acid; (d) C_{60}CHCOOH.

Figure 3. Influence of the cross flow rate on the apparent size of fullerene aggregates.

Figure 4. AF4-MALS fractograms of surface modified fullerenes. The line shows the 90° scattering intensity, the marks the values of the r_G. For experimental conditions see text. (a) $C_{60}(OH)_{24}$; (b) $C_{120}(OH)_{30}$; (c) C_{60}-pyrr tris acid; (d) C_{60}CHCOOH.

Figure 5. TEM pictures of fullerene aggregates. (a) $C_{60}(OH)_{24}$; (b) $C_{120}(OH)_{30}$; (c) C_{60}-pyrr tris acid; (d) C_{60}CHCOOH.

Figure 6. Effect of the salt concentration of the carrier solution on the aggregate sizes as measured by AF4-UV.

Figure 7. Effect of the salt concentration of the carrier solution on the aggregate sizes of $C_{60}(OH)_{24}$ as measured by AF4-MALS.

Figure 8. Effect of the salt concentration of the carrier solution on the recovery of carboxy-fullerenes.

Accepted Manuscript

ACCEPTED MANUSCRIPT

References

[1] H.W. Kroto, J.R. Heath, S.C. O'Brien, R.F. Curl, R.E. Smalley, C60: buckminsterfullerene, Nature 318 (1985) 162-163.

[2] D. Kronholm, J.C. Hummelen, Fullerene-based n-type semiconductors in organic electronics, Mater. Matters 2 (2007) 16-19.

[3] L. Xiao, H. Takada, K. Maeda, M. Haramoto, N. Miwa, Antioxidant effects of water-soluble fullerene derivatives against ultraviolet ray or peroxylipid through their action of scavenging the reactive oxygen species in human skin keratinocytes, Biomed. Pharmacother. 59 (2005) 351-358.

[4] N. Tagmatarchis, H. Shinohara, Fullerenes in medicinal chemistry and their biological applications, Mini-Rev. Med. Chem. 1 (2001) 339-348.

[5] R. Partha, J.L. Conyers, Biomedical applications of functionalized fullerene-based nanomaterials, Int. J. Nanomed. 4 (2009) 261-275.

[6] J. Li, A. Takeuchi, M. Ozawa, X. Li, K. Saigo, K. Kitazawa, C60 fullerol formation catalyzed by quaternary ammonium hydroxides, J. Chem. Soc. , Chem. Commun. (1993) 1784-1785.

[7] L.L. Dugan, J.K. Gabrielsen, S.P. Yu, T.S. Lin, D.W. Choi, Buckminsterfullerenol free radical scavengers reduce excitotoxic and apoptotic death of cultured cortical neurons, Neurobiol. Dis. 3 (1996) 129-135.

[8] D.M. Guldi, K.D. Asmus, Activity of water-soluble fullerenes towards Â·OH-radicals and molecular oxygen, Radiat. Phys. Chem. 56 (1999) 449-456.

[9] M. Prato, [60]Fullerene chemistry for materials science applications, J. Mater. Chem. 7 (1997) 1097-1109.

[10] X. Cai, H. Jia, Z. Liu, B. Hou, C. Luo, Z. Feng, W. Li, J. Liu, Polyhydroxylated fullerene derivative C60(OH)24 prevents mitochondrial dysfunction and oxidative damage in an MPP+-induced cellular model of Parkinson's disease, Journal of Neuroscience Research 86 (2008) 3622-3634.

[11] L. Dai, A.W.H. Mau, A facile route to fullerol-containing polymers, Synthetic Metals 86 (1997) 2277-2278.

[12] J. Yu, L. Dong, C. Wu, L. Wu, J. Xing, Hydroxyfullerene as a novel coating for solid-phase microextraction fiber with sol–gel technology, Journal of Chromatography A 978 (2002) 37-48.

[13] B. Sitharaman, S. Asokan, I. Rusakova, M.S. Wong, L.J. Wilson, Nanoscale Aggregation Properties of Neuroprotective Carboxyfullerene (C3) in Aqueous Solution, Nano Lett. 4 (2004) 1759-1762.

[14] H. Tokuyama, S. Yamago, E. Nakamura, T. Shiraki, Y. Sugiura, Photoinduced biochemical activity of fullerene carboxylic acid, J. Am. Chem. Soc. 115 (1993) 7918-7919.

[15] S.H. Friedman, D.L. DeCamp, R.P. Sijbesma, G. Srdanov, F. Wudl, G.L. Kenyon, Inhibition of the HIV-1 protease by fullerene derivatives: model building studies and experimental verification, J. Am. Chem. Soc. 115 (1993) 6506-6509.

[16] H. Kato, N. Shinohara, A. Nakamura, M. Horie, K. Fujita, K. Takahashi, H. Iwahashi, S. Endoh, S. Kinugasa, Characterization of fullerene colloidal suspension in a cell culture medium for in vitro toxicity assessment, Mol. BioSyst. 6 (2010) 1238-1246.

[17] K.W. Powers, M. Palazuelos, B.M. Moudgil, S.M. Roberts, Characterization of the size, shape, and state of

Accepted Manuscript

ACCEPTED MANUSCRIPT

dispersion of nanoparticles for toxicological studies, Nanotoxicoloxy 1 (2007) 42-51.

[18] D.Y. Lyon, L.K. Adams, J.C. Falkner, P.J.J. Alvarez, Antibacterial activity of fullerene water suspensions: Effects of preparation method and particle size, Environ. Sci. Technol. 40 (2006) 4360-4366.

[19] R.D. Handy, R. Owen, E. Valsami-Jones, The ecotoxicology of nanoparticles and nanomaterials: current status, knowledge gaps, challenges, and future needs, Ecotoxicology 17 (2008) 315-325.

[20] S.J. Klaine, P.J.J. Alvarez, G.E. Batley, T.F. Fernandes, R.D. Handy, D.Y. Lyon, S. Mahendra, M.J. McLaughlin, J.R. Lead, Nanomaterials in the environment: behavior, fate, bioavailability, and effects, Environ. Toxicol. Chem. 27 (2008) 1825-1851.

[21] C.F. Jones, D.W. Grainger, In vitro assessments of nanomaterial toxicity, Adv. Drug Delivery Rev. 61 (2009) 438-456.

[22] J. Demeester, S.S. De Smedt, N.N. Sanders, J.Haustraete, Light scattering, in: W. Jiskoot, D.J. Crommelin (Eds.), Methods for structural analysis of protein pharmaceuticals, AAPS Press, Arlington, 2005, pp. 245-275

[23] S.M. Brar, M. Verma, Measurement of nanoparticles by light-scattering techniques, TrAC 30 (2011) doi:10.1016/j.trac.2010.08.008-

[24] J.C. Giddings, F.J. Yang, M.N. Mayers, Theoretical and experimental characterization of flow field-flow fractionation, Anal. Chem. 48 (1976) 1126-1132.

[25] K.G. Wahlund, Flow field-flow fractionation: Critical overview, J. Chromatogr. A 1287 (2013) 97-112.

[26] K.G. Wahlund, J.C. Giddings, Properties of an asymmetrical flow field-flow fractionation channel having one permeable wall, Anal. Chem. 59 (1987) 1332-1339.

[27] M. E. Schimpf, C.K. Caldwell, J.C. Giddings, Field Flow Fractionation Handbook, John Wiley & Sons, New York, 2000

[28] K.G. Wahlund, Improved terminology for experimental field-flow fractionation, Anal. Bioanal. Chem. 406 (2014) 1579-1583.

[29] M. Baalousha, B. Stolpe, J.R. Lead, Flow field-flow fractionation for the analysis and characterization of natural colloids and manufactured nanoparticles in environmental systems: a critical review., J. Chromatogr. A 1218 (2011) 4078-4103.

[30] C.J. Giddings, Field-flow fractionation: analysis of macromolecular, colloidal, and particulate materials, Science 260 (1993) 1456-1466.

[31] C.J. Giddings, M.N. Myres, Steric field-flow fractionation: a new method for separating 1-100 um particles, Separat. Sci. Technol. 13 (1978) 637-645.

[32] M.N. Myres, C.J. Giddings, Properties of the transition from normal to steric field-flow fractionation, Anal. Chem. 54 (1982) 2284-2289.

[33] C.W. Isaacson, D. Bouchard, Asymmetric flow field flow fractionation of aqueous C60 nanoparticles with size determination by dynamic light scattering and quantification by liquid chromatography atmospheric pressure photo-ionization mass spectrometry, J. Chromatogr. , A 1217 (2010) 1506-1512.

[34] S. Assemi, S. Tadjiki, B.C. Donose, A.V. Nguyen, J.D. Miller, Aggregation of Fullerol C60(OH)24 Nanoparticles as Revealed Using Flow Field-Flow Fractionation and Atomic Force Microscopy, Langmuir

Accepted Manuscript

ACCEPTED MANUSCRIPT

26 (2010) 16063-16070.

[35] P. Herrero, P.S. Baeuerlein, E. Emke, E. Pocurull, P. de Voogt, Asymmetrical flow field-flow fractionation hyphenated to Orbitrap high resolution mass spectrometry for the determination of (functionalised) aqueous fullerene aggregates, J. Chromatogr. A 1356 (2014) 277-282.

[36] P. Herrero, P.S. Baeuerlein, E. Emke, R.M. Marcé, P. de Voogt, Size and concentration determination of (functionalised) fullerenes in surface and sewage water matrices using field flow fractionation coupled to an online accurate mass spectrometer: Method development and validation, Anal. Chim. Acta 851 (2015) 77-84.

[37] J.A. Brant, J. Labille, C.O. Robichaud, M. Wiesner, Fullerol cluster formation in aqueous solutions: Implications for environmental release, J. Colloid Interface Sci. 314 (2007) 281-288.

[38] G.V. Andrievsky, M.V. Kosevich, O.M. Vovk, V.S. Shelkovsky, L.A. Vashchenko, On the production of an aqueous colloidal solution of fullerenes, J. Chem. Soc. , Chem. Commun. (1995) 1281-1282.

[39] A. Litzén, Separation Speed, Retention, and Dispersion in Asymmetrical Flow Field-Flow Fractionation as Functions of Channel, Dimensions and Flow rates, Anal. Chem. 65 (1993) 461-470.

[40] K.G. Wahlund, H.S. Winegarner, K.D. Caldwell, J.C. Giddings, Improved flow field-flow fractionation system applied to water-soluble polymers: programming, outlet stream splitting, and flow optimization, Anal. Chem. 58 (1986) 573-578.

[41] V. Georgakilas, F. Pellarini, M. Prato, D.M. Guldi, M. Melle-Franco, F. Zerbetto, Supramolecular self-assembled fullerene nanostructures, Proc. Natl. Acad. Sci. U. S. A. 99 (2002) 5075-5080.

[42] J. Cho, G. Amy, J. Pellegrino, Membrane filtration of natural organic matter: initial comparison of rejection and flux decline characteristics with ultrafiltration and nanofiltration membranes, Water Res. 33 (1999) 2517-2526.

[43] J. Cho, G. Amy, J. Pellegrino, Membrane filtration of natural organic matter: factors and mechanisms affecting rejection and flux decline with charged ultrafiltration (UF) membrane, J. Membrane Sci. 164 (2000) 89-110.

[44] R.L. Hartmann, R.S.K. Williams, Flow field-flow fractionation as an analytical technique to rapidly quantitate membrane fouling, J. Membrane Sci. 209 (2002) 93-106.

[45] Y. Kiso, Y. Sugiura, T. Kitao, K. Nishimura, Effects of hydrophobicity and molecular size on rejection of aromatic pesticides with nanofiltration membranes, Journal of Membrane Science 192 (2001) 1-10.

[46] M.N. Thang, H. Geckeisa, J.I. Kim, H.P. Beck, Application of the flow field flow fractionation (FFFF) to the characterization of aquatic humic colloids: evaluation and optimization of the method, Colloids and Surfaces A: Physicochemical and Engineering Aspects 181 (2001) 289-301.

[47] J.F. Blanco, J. Sublet, Q.T. Nguyen, P. Schaetzel, Formation and morphology studies of different polysulfone-based membranes made by wet phase inversion process, Journal of Membrane Science 283 (2006) 27-37.

[48] M. Baalousha, M. Motelica-Heino, P. Le Coustumera, Conformation and size of humic substances: Effects of major cation concentration and type, pH, salinity, and residence time, Colloids and Surfaces A: Physicochemical and Engineering Aspects 272 (2006) 48-55.

[49] M.R. Schure, S.A. Palkar, Accuracy estimation of multiangle light scattering detectors utilized for polydisperse particle characterization with field-flow fractionation techniques: a simulation study, Anal.

ACCEPTED MANUSCRIPT

Chem. 74 (2002) 684-695.

[50] J.D. Fortner, D.Y. Lyon, C.M. Sayes, A.M. Boyd, J.C. Falkner, E.M. Hotze, L.B. Alemany, Y.J. Tao, W. Guo, K.D. Ausman, V.L. Colvin, J.B. Hughes, C60 in Water: Nanocrystal Formation and Microbial Response, Environ. Sci. Technol. 39 (2005) 4307-4316.

[51] J. Brant, H. Lecoanet, M.R. Wiesner, Aggregation and deposition characteristics of fullerene nanoparticles in aqueous systems, J. Nanopart. Res. 7 (2005) 545-553.

[52] B. Derjaguin, L. Landau, Theory of the stability of strongly charged lyophobic sols and of the adhesion of strongly charged particles in solutions of electrolytes, Acta Physicochim. URSS 14 (1941) 633-662.

[53] G. Karaiskakis, M. Douma, I. Katsipou, A. Koliadima, L. Farmakis, Study of the recovery of colloidal particles in potential barrier sedimentation field-flow fractionation, J. Liq. Chromatogr. & Relat. Technol. 23 (2000) 1953-1959.

[54] N. Lioris, A. Farmakis, A. Koliadima, G. Karaiskakis, Estimation of the particle-wall interaction energy in sedimentation field-flow fractionation, J. Chromatogr. A 1087 (2005) 13-19.

[55] L. Pasol, M. Martin, M.L. Ekiel-Jezwska, E. Wajnryb, J. Blawzdziewicz, F. Feullebois, Motion of a sphere parallel to plane walls in a Poiseuille flow. Application to field-flow fractionation and hydrodynamic chromatography, Chem. Eng. Sci. 66 (2011) 4078-4089.

[56] A. Ulrich, S. Losert, N. Bendixen, A. Al-Kattan, H. Hagendorfer, B. Nowack, C. Adlhart, J. Ebert, M. Lattuadae, K. Hungerbuhler, Critical aspects of sample handling for direct nanoparticle analysis and analytical challenges using asymmetric field flow fractionation in a multi-detector approach, J. Anal. At. Spectrom. 27 (2012) 1120-1130.

[57] S. Schachermeyer, J. Ashby, M. Kwon, W. Zhong, Impact of Carrier Fluid Composition on Recovery of Nanoparticles and Proteins in Flow Field Flow Fractionation, J. Chromatogr. , A 1264 (2012) 72-79.

Accepted Manuscript

Figure 1
Click here to download high resolution image

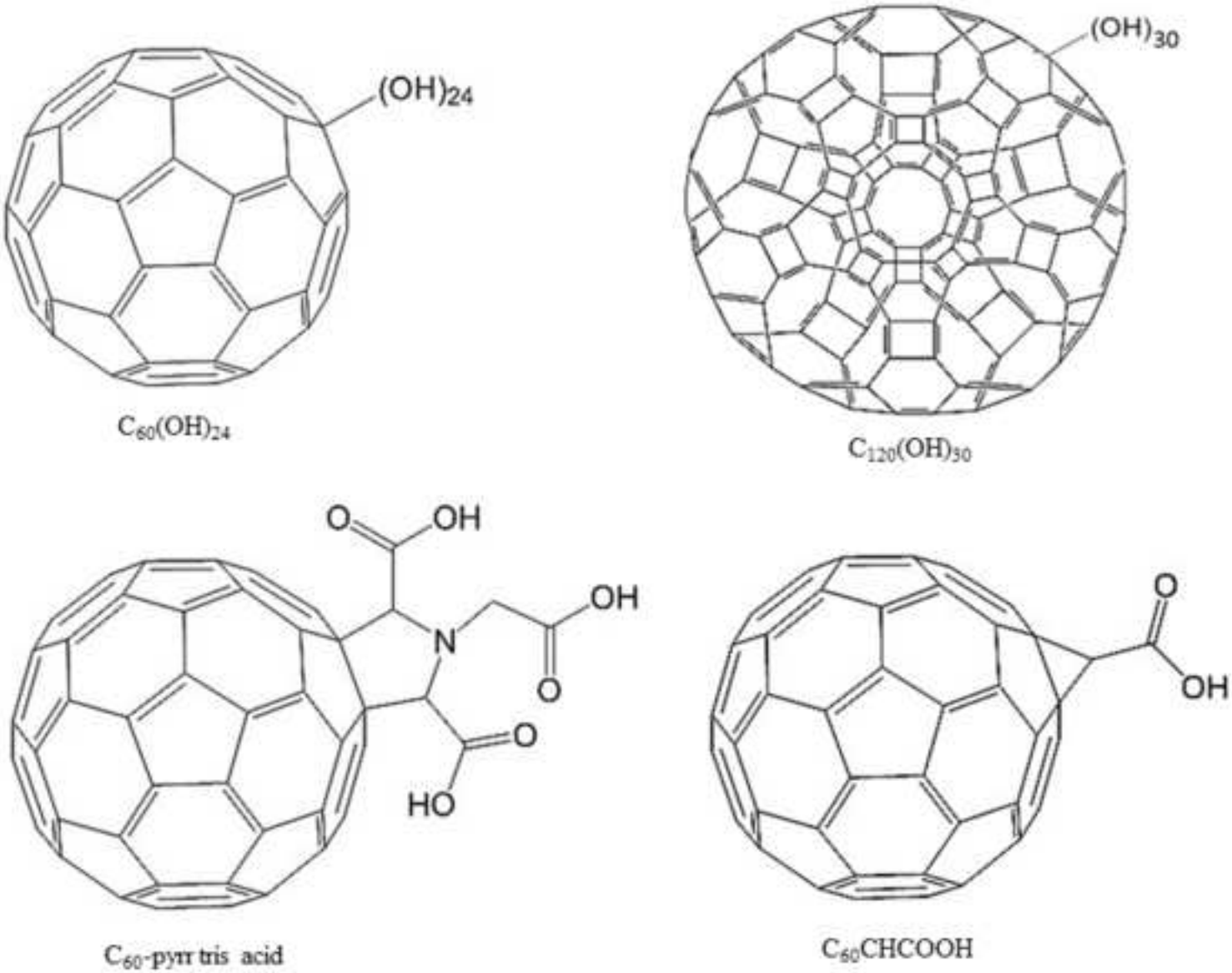

Figure 2

Click here to download high resolution image

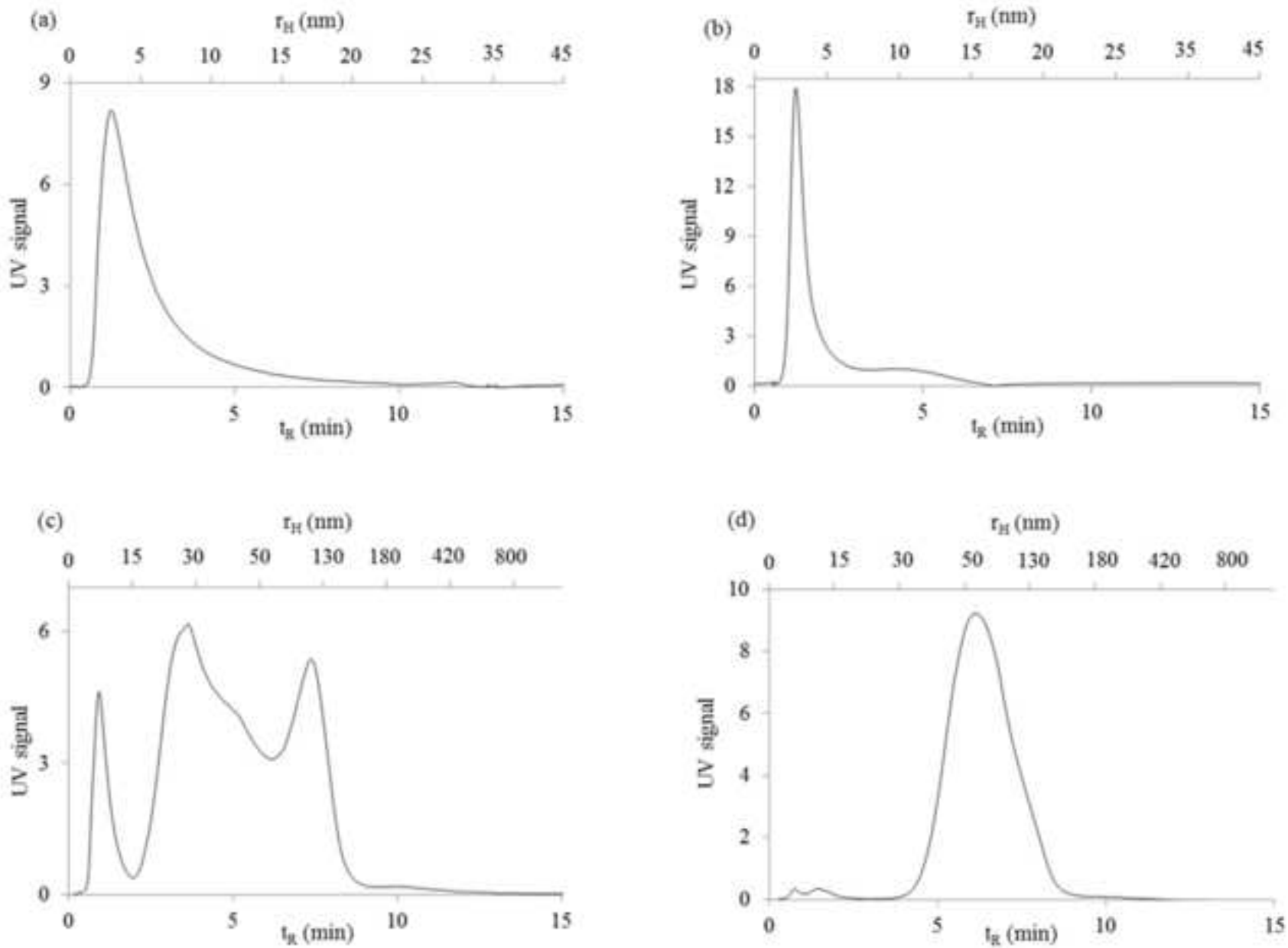

Figure 3

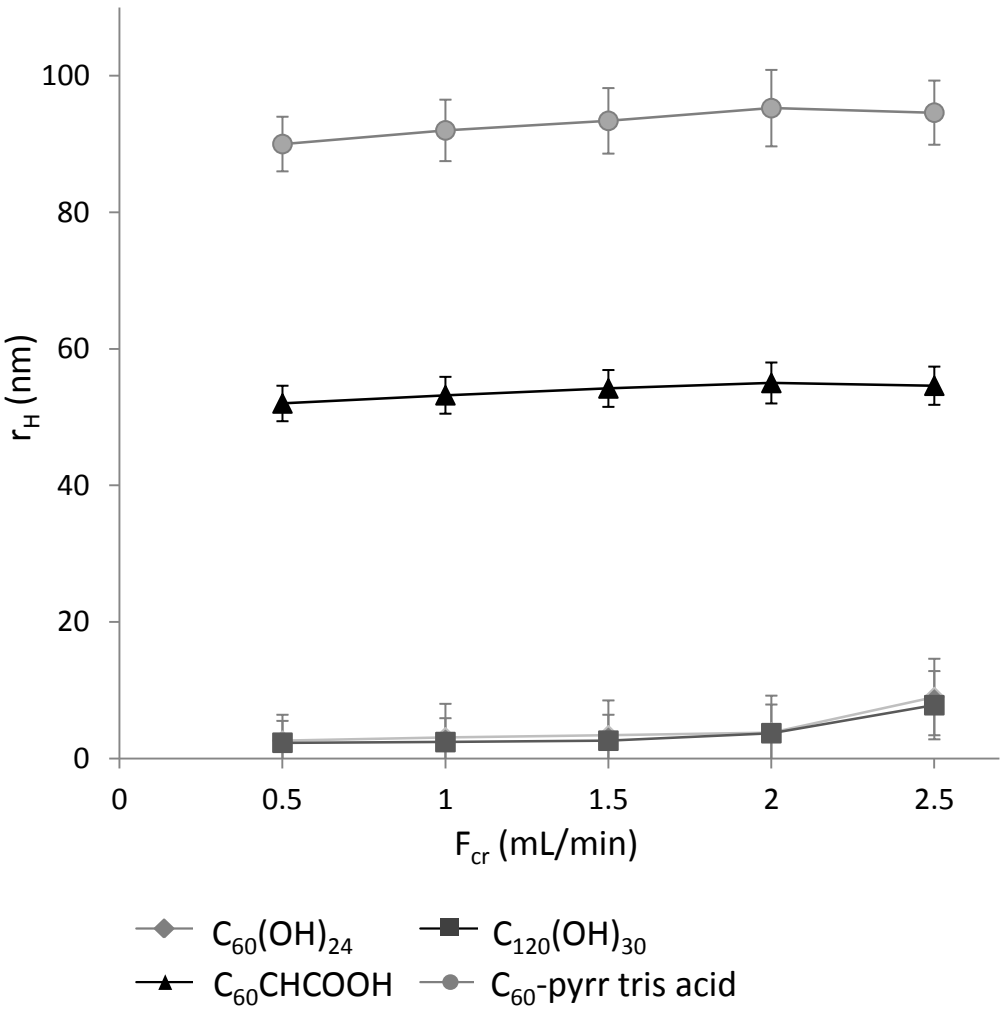
100
80
60
40
20
0
r_H (nm)
0
0.5
1
1.5
2
2.5
F_{cr} (mL/min)
$C_{60}(OH)_{24}$
$C_{120}(OH)_{30}$
$C_{60}CHCOOH$
C_{60}-pyrr tris acid

Figure 4
Click here to download high resolution image

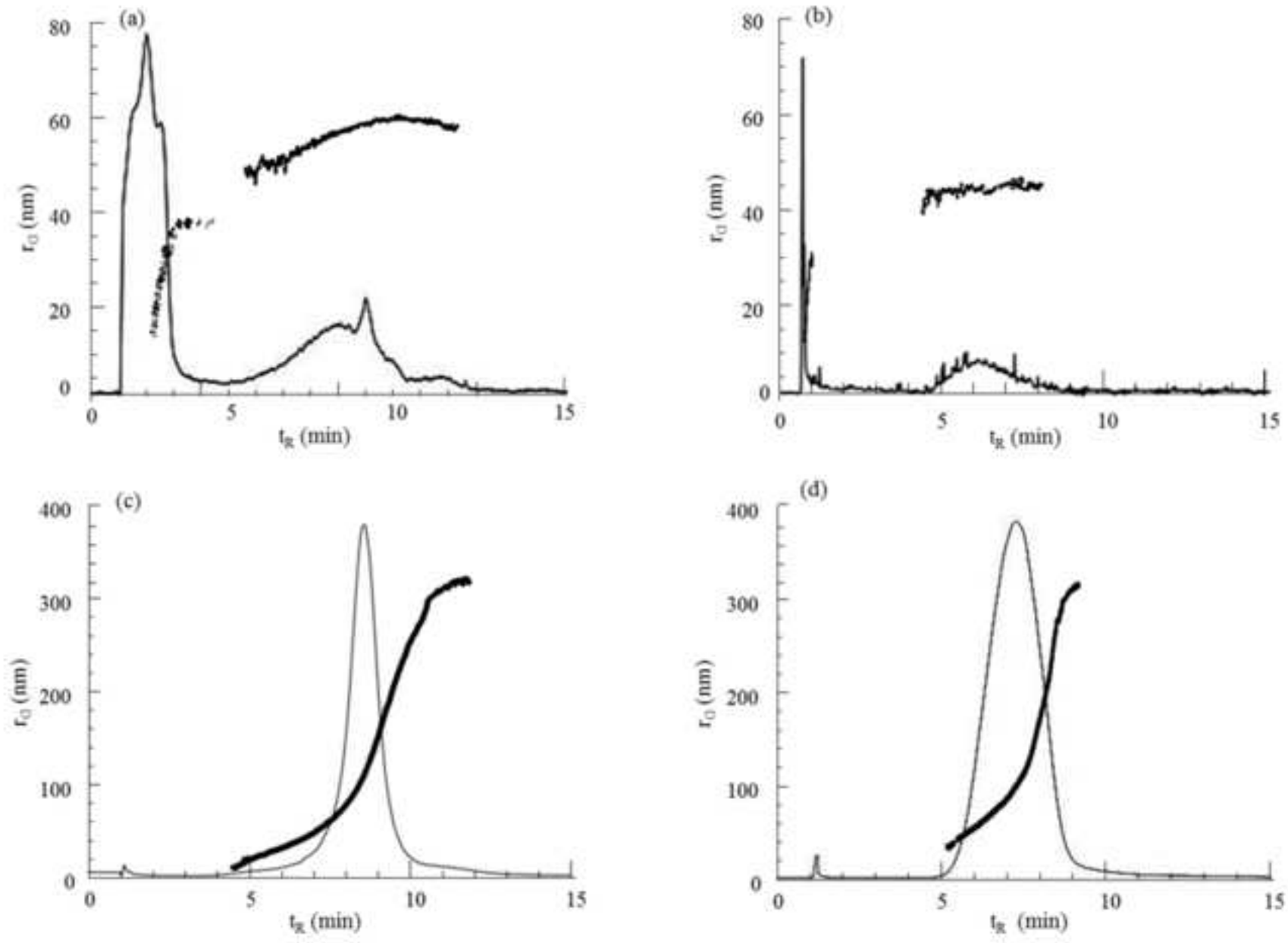

Figure 5
Click here to download high resolution image

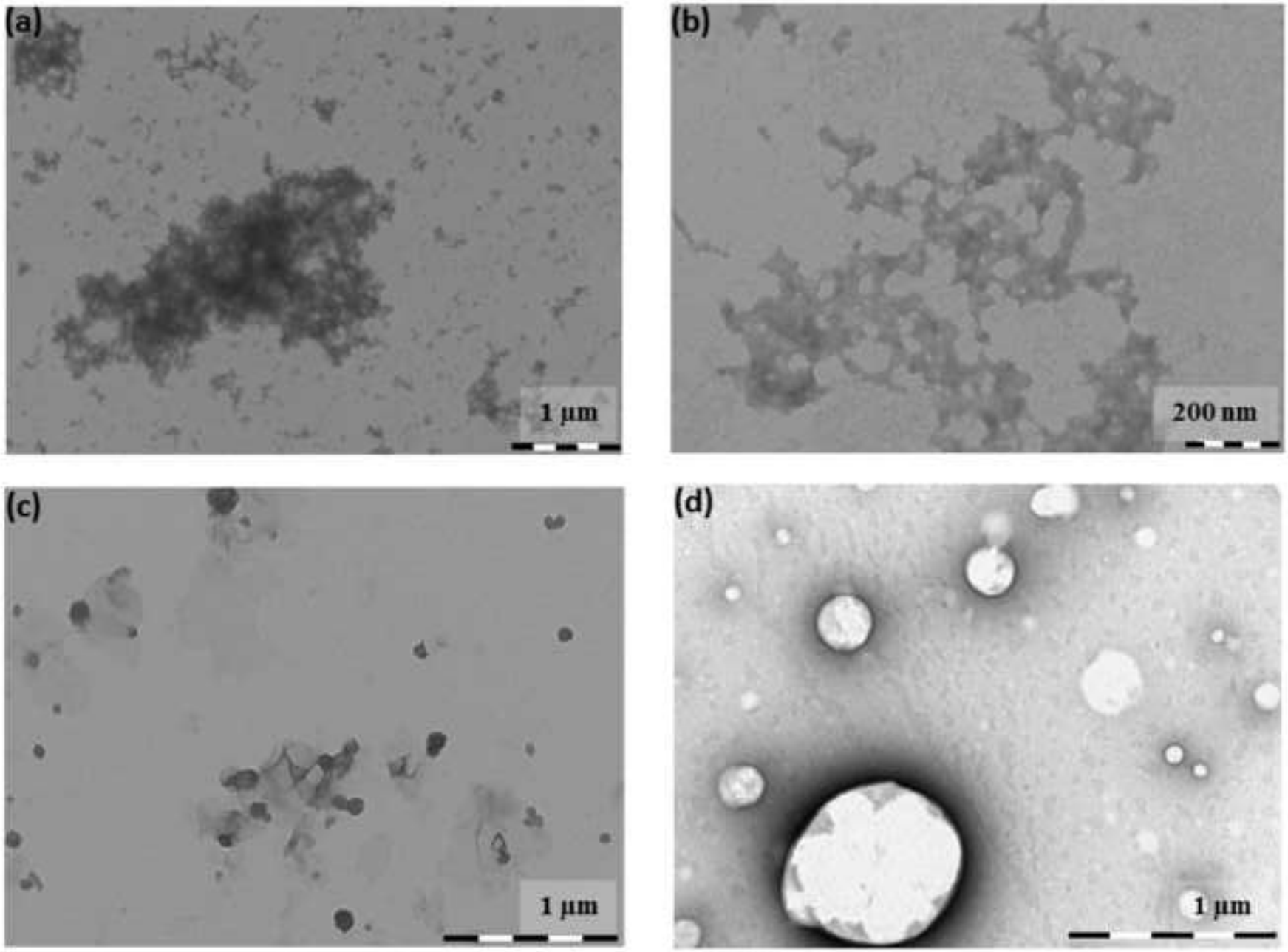

Figure 6

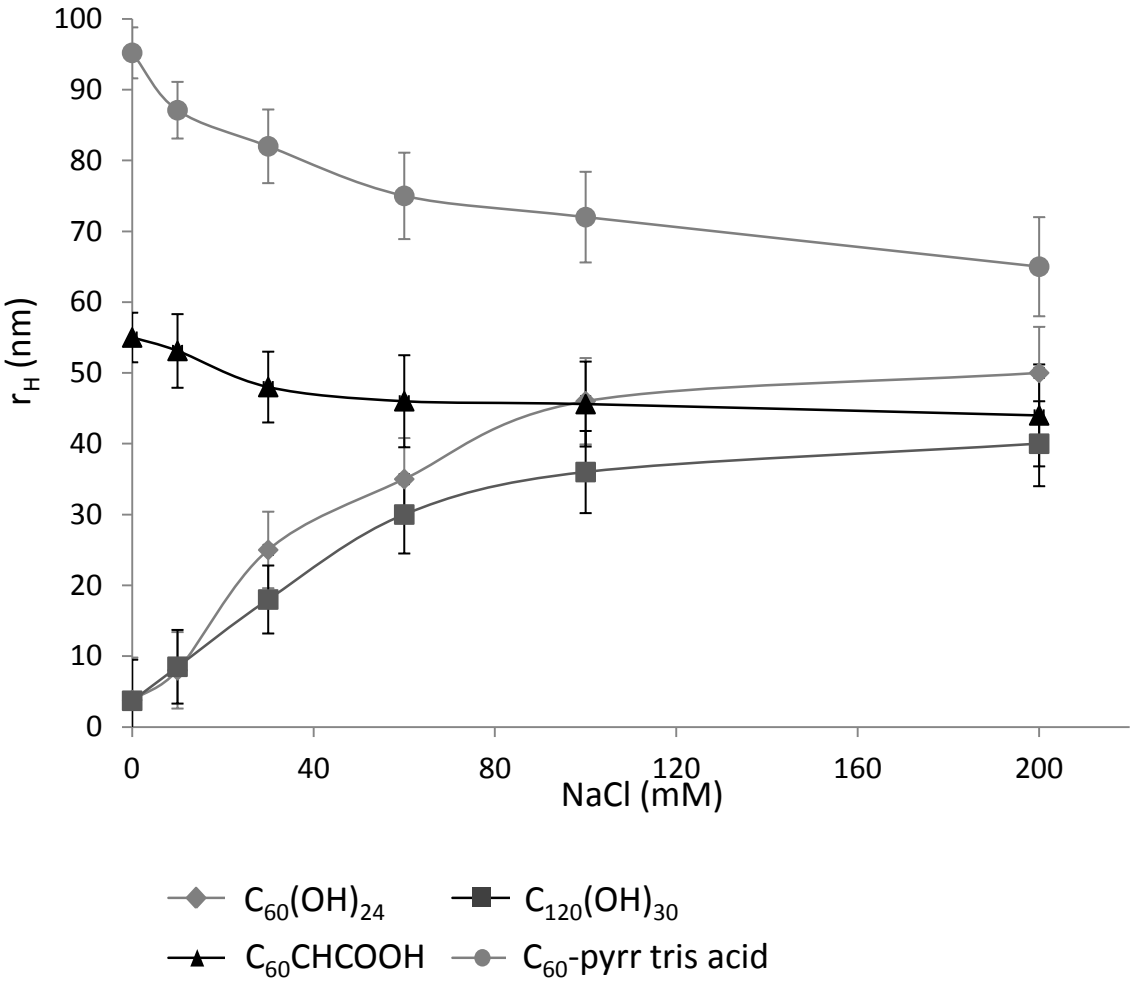
100
90
80
70
60
50
40
30
20
10
0
r_H (nm)
0
40
80
120
160
200
NaCl (mM)
$C_{60}(OH)_{24}$
$C_{120}(OH)_{30}$
$C_{60}CHCOOH$
C_{60}-pyrr tris acid

Figure 7
Click here to download high resolution image

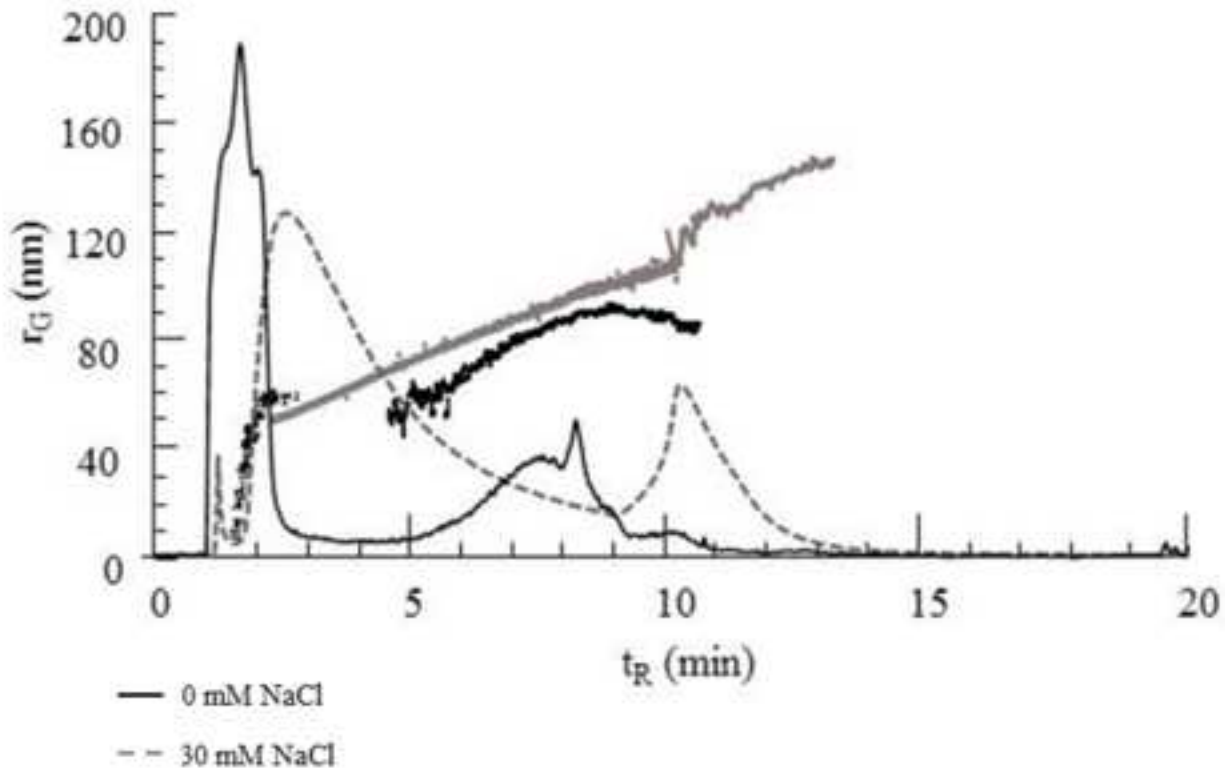

Figure 8
Click here to download high resolution image

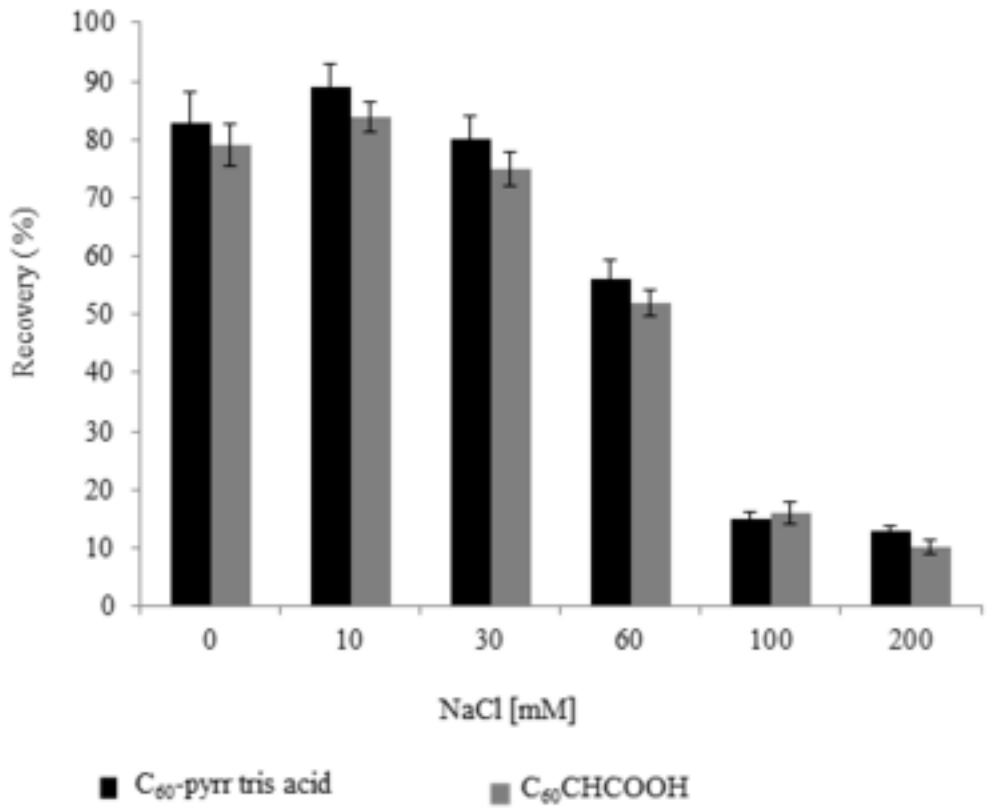

ACCEPTED MANUSCRIPT

Table 1. Recoveries of surface modified fullerenes from the AF4 channel using different membrane materials.

Membrane, cutoff	**Recovery± S.D. (%)**			
	$C_{60}(OH)_{24}$	**$C_{120}(OH)_{30}$**	**C_{60}-pyrr tris acid**	**$C_{60}CHCOOH$**
RC, 10 kDa	85 ± 4.1	87 ± 3.5	83 ± 5.0	79 ± 3.6
PES, 10 kDa	88 ± 3.0	85 ± 4.5	76 ± 5.7	73 ± 4.0
RC, 3 kDa	83 ± 3.7	85 ± 4.0	79 ± 3.3	76 ± 4.8
PES, 3 kDa	83 ± 5.3	87 ± 2.4	75 ± 3.1	70 ± 6.8

Accepted Manuscript